

SUPPLEMENTAL FIGURES & TABLES: Species' Sensitivity to Hydrologic Whiplash in The Tree-Ring Record of the High Sierra Nevada

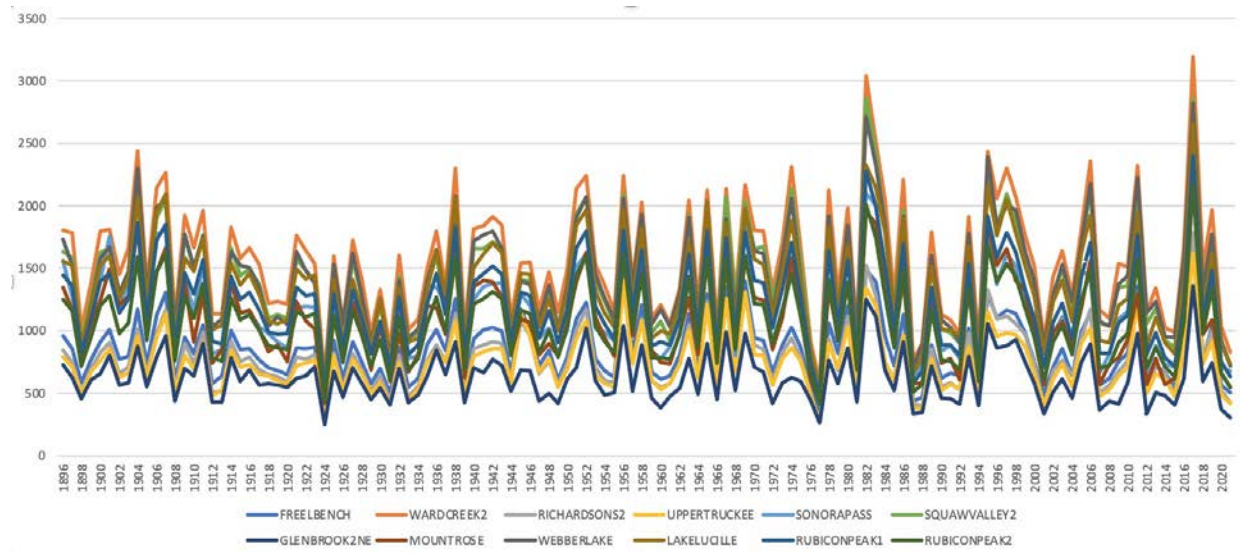


Figure S1. Time series of PRISM water-year precipitation at 12 SWE monitoring stations, 1896-2020. Site names correspond to sites listed at <https://cdec.water.ca.gov/> (accessed on 2 February 2022).

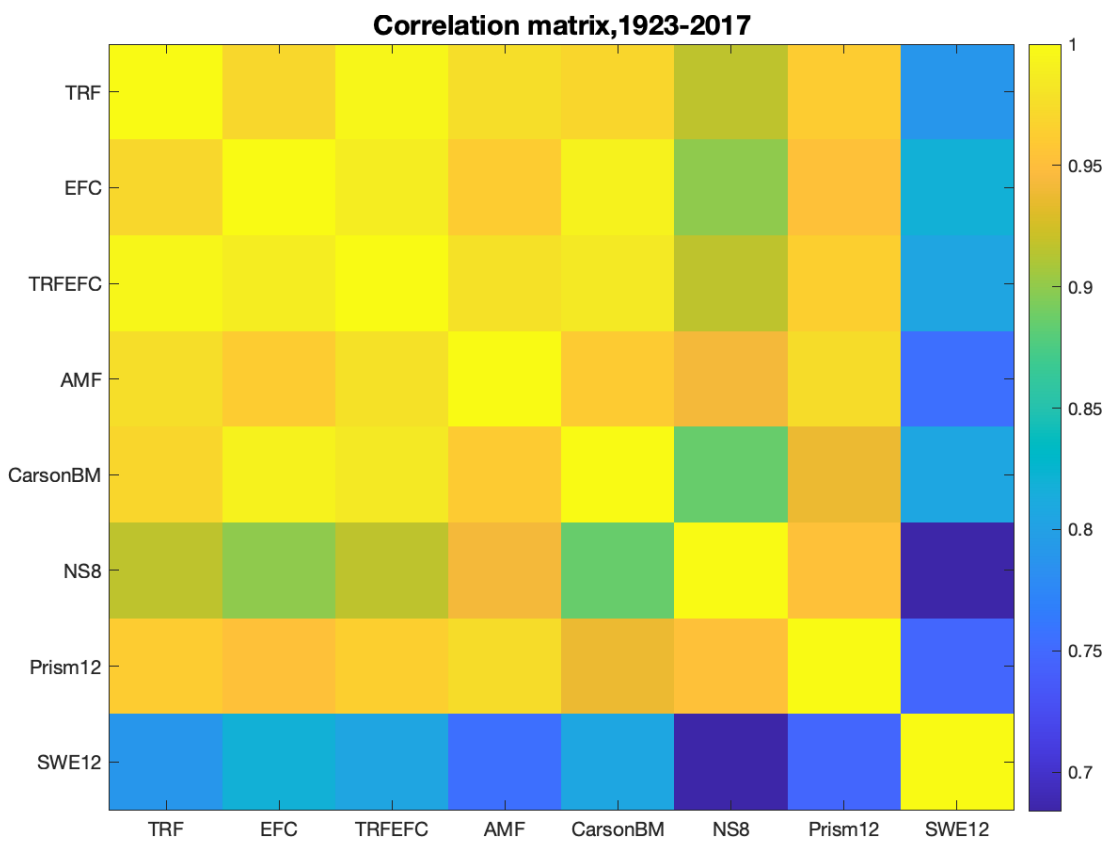


Figure S2. Correlation matrix of annual hydroclimatic series, 1923–2017. Site codes are defined in Table S1.

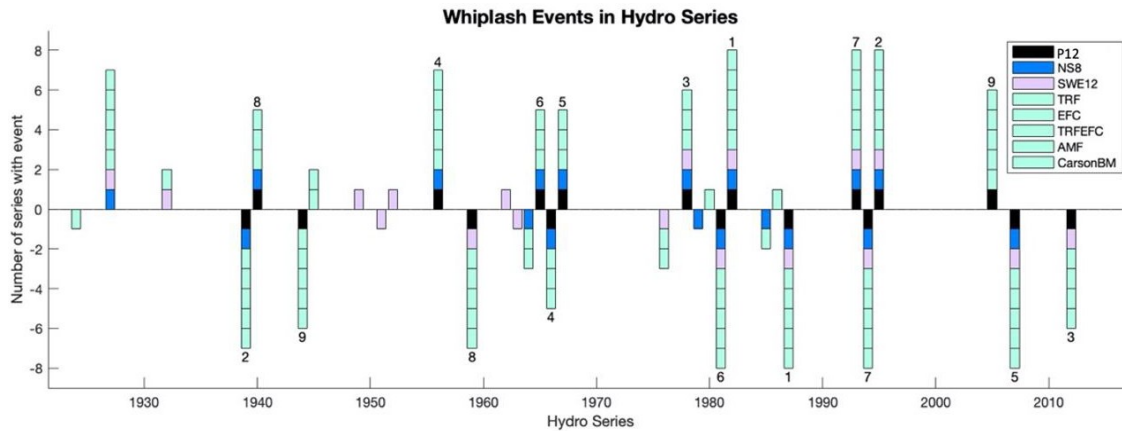


Figure S3. Synchrony of positive whiplash events in alternative annual hydroclimatic series, 1923–2017. The top eight ranked whiplash events in each series are represented in the plot. Numbers indicate the event ranking of P12 events. P12 whiplash events are coded in black, the Northern Sierra 8-Station Precipitation Index (NS8) in blue, the Snow Water Equivalent (SWE12) in light purple, and 5 streamflows (natural flows) in light blue-green. Site codes are defined in Table S1.

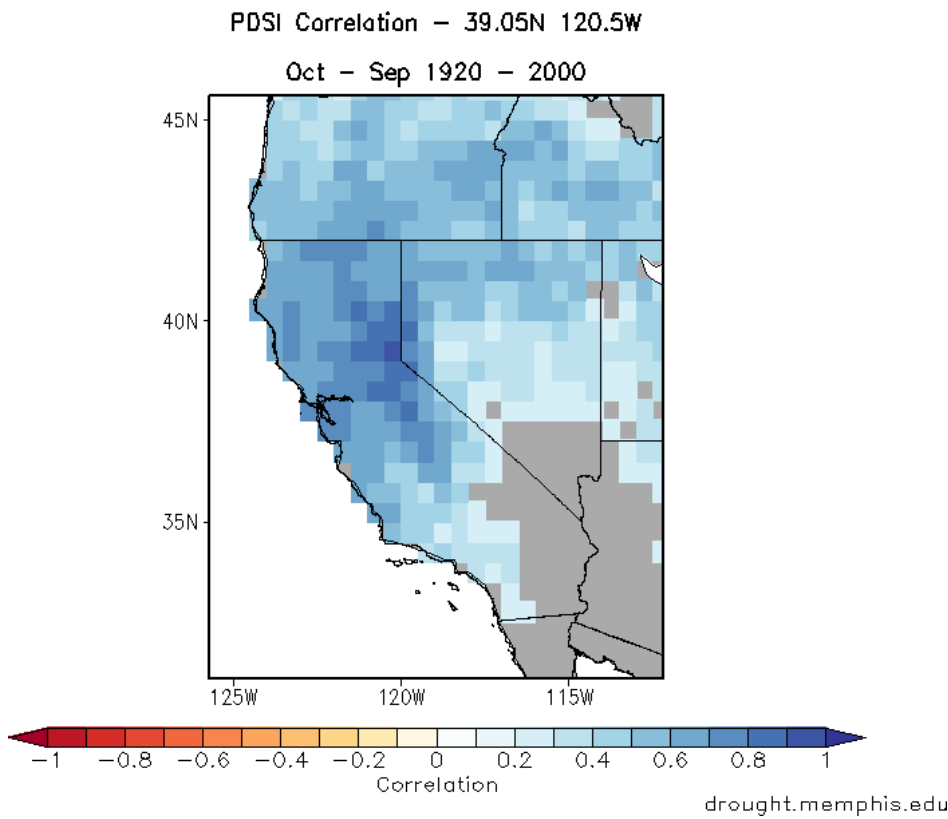


Figure S4. The climate footprint of the Truckee-Carson River Basin is illustrated with the spatial correlation of the instrumental summer (June-July-August) Palmer Drought Severity Index (PDSI) on a 0.5-degree latitude-longitude grid. The correlations are with the point over the basin. Analysis period: 1920-2000. Map generated at <http://drought.memphis.edu/NADA/Correlation.aspx> (accessed on 13 January 2021).

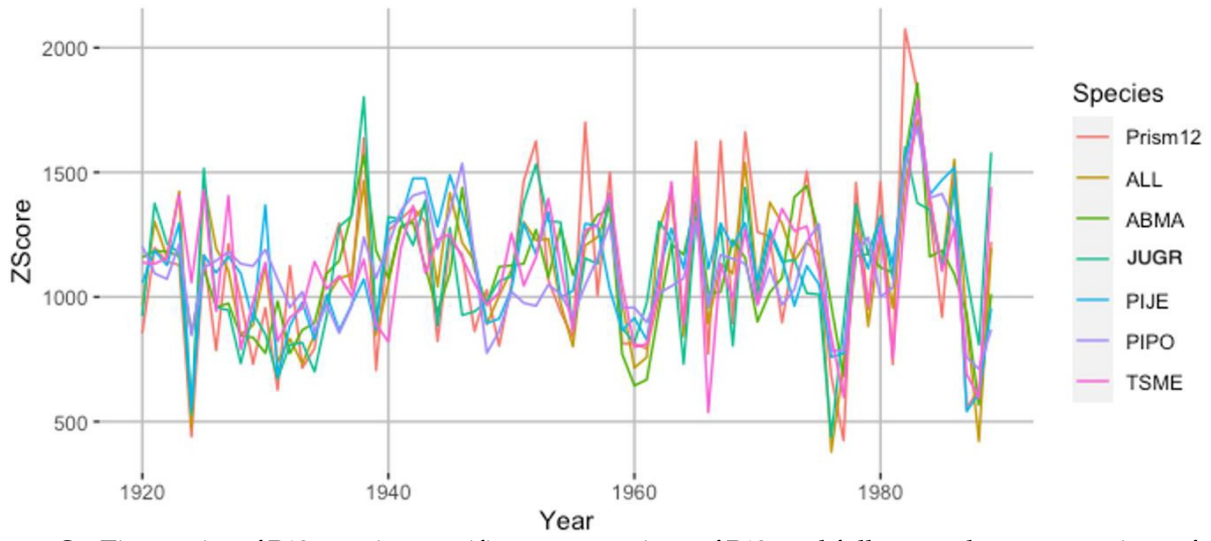


Figure S5. Time series of P12, species-specific reconstructions of P12, and full-network reconstructions of P12.

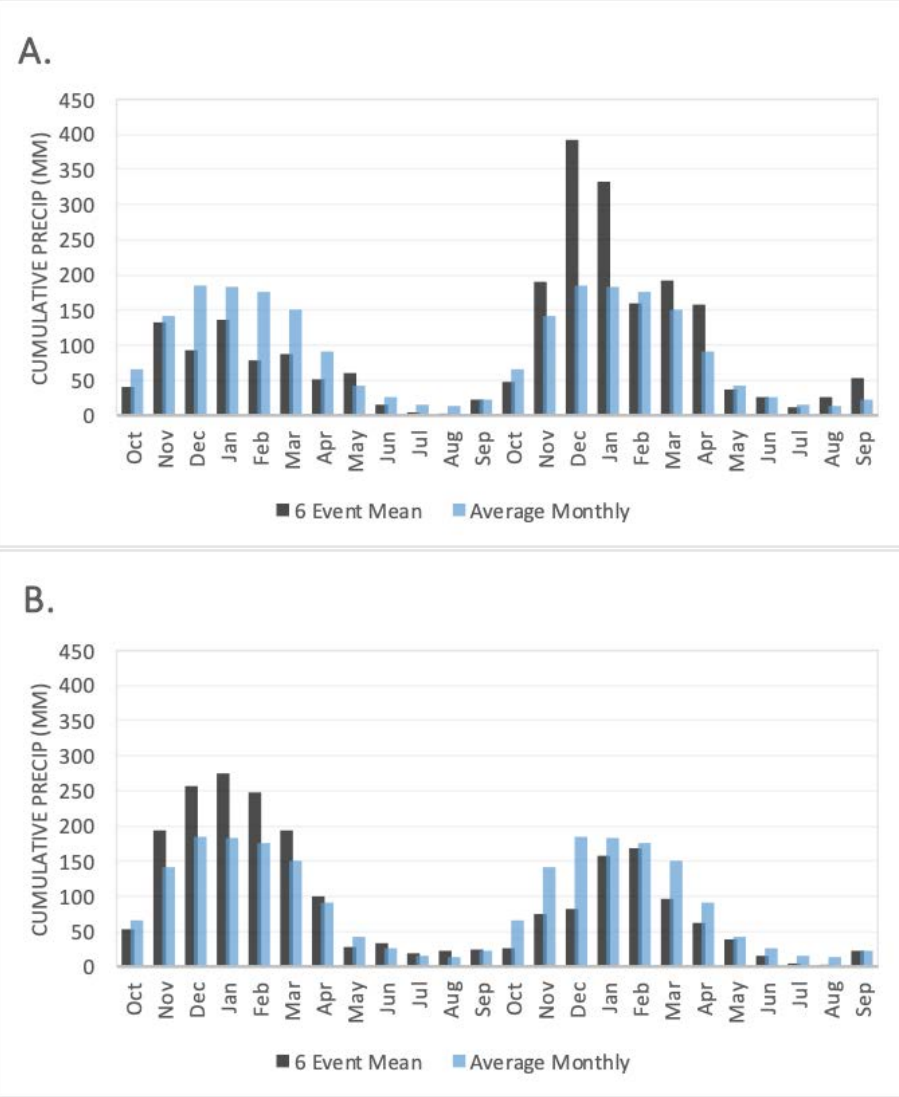


Figure S6. Mean of monthly P12 precipitation in years of whiplash events in P12. **(A)** Positive events. **(B)** Negative events. Blue shows the long-term mean monthly precipitation, which does not vary among frames.

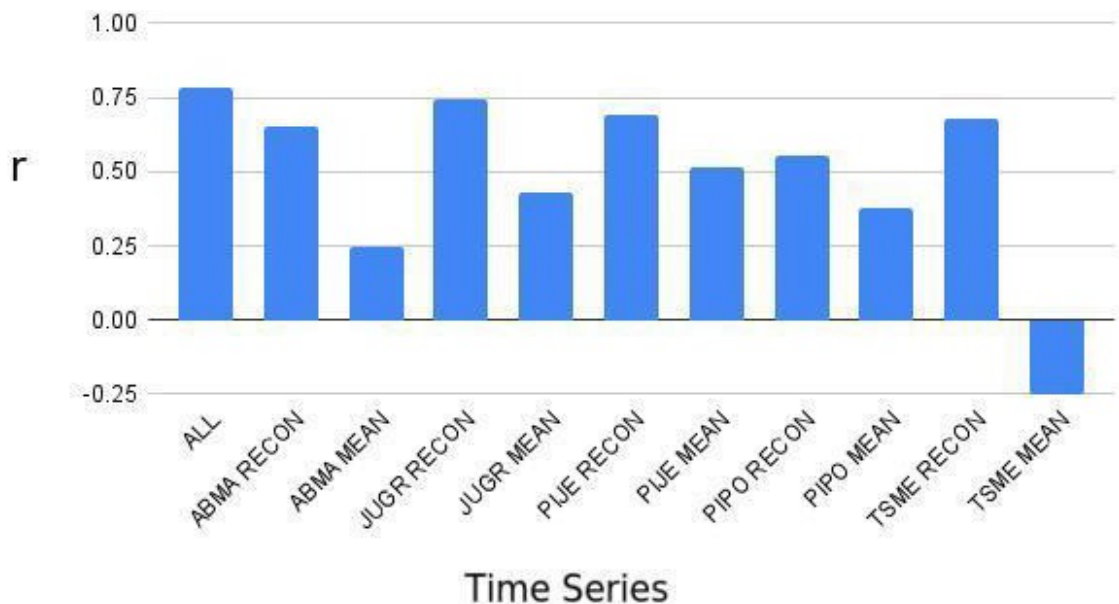


Figure S7. Correlation of annual precipitation (P12) with species-mean chronologies and with full-network (All) and species-specific reconstructions, 1920-1989. For reconstructions, the squared r is equivalent to the regression R-squared of the reconstruction models reported in this paper. For the mean chronologies, squared r is equivalent to the regression R-squared of a simple linear regression model of P12 on the mean of available chronologies (no screening, no lags) of a particular species. Note the negative ($r=-0.25$) correlation for TSME MEAN. A simple linear regression model of P12 on that mean chronology would explain 6.25% (-0.25 squared) of the variance of P12. The model would have a negative regression coefficient, reflecting the tendency for heavy snowpack to be associated with a narrow ring in mountain hemlock in the current year.

Table S1. Key for 8 Hydroclimatic series in/near the Truckee-Carson River Basin. Time series for analyses are annual (average or sum of water year is from October to September), except for SWE12, a measure of April 1st Snow Water Equivalent.

| ID | TYPE | UNITS | SOURCE | NAME |
|----------|------|---------|--------|--|
| TRF | FNF | mcm | CDEC | Truckee River at Farad |
| EFC | FNF | mcm | CDEC | East Fork Carson River nr Garnerville |
| TRFEFC | FNF | mcm | CDEC | Sum of Truckee and E Fork Carson |
| AMF | FNF | mcm | CDEC | American River at Folsom |
| CARSONBM | FLO | Z-score | USGS | Carson River calibration series (Biondi and Meko 2019) |
| NS8 | PCP | mm | CDEC | Northern Sierra 8-Station Precipitation Index |
| PRISM12 | PCP | mm | PRISM | PRISM precipitation averaged over points for SWE12 |
| SWE12 | Snow | %normal | CDEC+ | 12-station snow-course SWE assembled by us |

Table S2. Summary statistics of site-specific reconstructions of P12. Statistics in columns are the same as in Table 2.

| Recon | Species Code | Lags Used | R ² | R ² adj | F | pF | REcv | RSME |
|---------------|--------------|-----------|----------------|--------------------|--------|------------------------|--------|---------|
| CA574 | ABMA | P1 | 0.287 | 0.266 | 13.294 | 1.41×10^{-5} | 0.261 | 302.415 |
| CA589 | ABMA | | 0.069 | 0.055 | 4.957 | 2.93×10^{-2} | 0.034 | 345.857 |
| CA691 | ABMA | | 0.267 | 0.259 | 33.455 | 9.95×10^{-8} | 0.261 | 299.090 |
| CA696 | ABMA | | 0.228 | 0.219 | 26.838 | 1.32×10^{-6} | 0.209 | 310.652 |
| CA630 | JUGR | N2 P2 | 0.062 | 0.024 | 1.639 | 1.88×10^{-1} | 0.040 | 350.903 |
| CA631 | JUGR | N1 | 0.018 | -0.008 | 0.679 | 5.10×10^{-1} | -0.019 | 361.530 |
| CA632 | JUGR | N2 | 0.184 | 0.162 | 8.440 | 4.94×10^{-4} | 0.171 | 326.115 |
| CA698 | JUGR | | 0.016 | 0.006 | 1.516 | 2.21×10^{-1} | -0.007 | 350.564 |
| DGS | JUGR | | 0.419 | 0.411 | 56.186 | 8.86×10^{-11} | 0.401 | 276.270 |
| IVJ | JUGR | N2 P2 | 0.114 | 0.079 | 3.227 | 2.72×10^{-2} | 0.073 | 345.360 |
| KAIM | JUGR | | 0.246 | 0.238 | 28.765 | 6.52×10^{-7} | 0.238 | 304.419 |
| CA677 | PIJE | N1 | 0.419 | 0.405 | 30.988 | 7.33×10^{-11} | 0.395 | 272.539 |
| CA678 | PIJE | | 0.282 | 0.274 | 34.245 | 8.39×10^{-8} | 0.282 | 296.951 |
| DLB | PIJE | | 0.028 | 0.015 | 2.179 | 1.44×10^{-1} | 0.008 | 357.126 |
| IVP | PIJE | | 0.025 | 0.012 | 1.935 | 1.68×10^{-1} | -0.010 | 360.491 |
| LEM | PIJE | P1 N1 | 0.157 | 0.130 | 5.880 | 1.00×10^{-3} | 0.129 | 338.129 |
| LSF | PIJE | P1 | 0.278 | 0.263 | 18.478 | 1.63×10^{-7} | 0.259 | 311.872 |
| LTV | PIJE | | 0.028 | 0.018 | 2.797 | 9.77×10^{-2} | 0.003 | 361.876 |
| SSP | PIJE | P1 | 0.361 | 0.344 | 21.174 | 5.12×10^{-8} | 0.335 | 292.021 |
| CA578 | PIPO | P2 N1 N2 | 0.418 | 0.382 | 11.491 | 4.32×10^{-7} | 0.361 | 281.239 |
| CA583 | PIPO | P1 N1 | 0.083 | 0.041 | 1.970 | 1.27×10^{-1} | 0.029 | 346.681 |
| CA694 | PIPO | P1 N1 | 0.211 | 0.185 | 7.938 | 9.48×10^{-5} | 0.155 | 321.127 |
| CA695 | PIPO | P1 N1 | 0.159 | 0.130 | 5.599 | 1.46×10^{-3} | 0.112 | 329.121 |
| CPRMTR | PIPO | P1 N1 | 0.175 | 0.149 | 6.719 | 3.68×10^{-4} | 0.145 | 335.146 |
| NOD | PIPO | | 0.006 | -0.007 | 0.449 | 5.05×10^{-1} | -0.019 | 357.991 |
| CA576 | TSME | P1 N2 N1 | 0.430 | 0.395 | 12.079 | 2.25×10^{-7} | 0.342 | 285.386 |
| CA692 | TSME | P1 N2 | 0.469 | 0.451 | 26.495 | 2.26×10^{-12} | 0.429 | 262.994 |
| GPH | TSME | P1 P2 | 0.211 | 0.180 | 6.701 | 4.56×10^{-4} | 0.169 | 326.904 |

Table S3. Significance of tracking of whiplash events in P12 by site-specific reconstructions as estimated by hypergeometric test. Sample size ($N_s = 69$) and maximum possible event matches ($M=6$) are the same for all reconstructions. The last two columns list the probability, by chance alone, of Q-or-more successes (events identified) given k draws from the sample.

| NAME | SPECIES CODE | Q (POS) | Q (NEG) | K (POS) | K (NEG) | P-VAL (POS) | P-VAL (NEG) |
|--------|--------------|---------|---------|---------|---------|-----------------------|-----------------------|
| CA574 | ABMA | 0 | 2 | 6 | 6 | 4.33×10^{-1} | 6.87×10^{-3} |
| CA589 | ABMA | 1 | 1 | 6 | 6 | 8.14×10^{-2} | 8.14×10^{-2} |
| CA691 | ABMA | 2 | 2 | 7 | 6 | 1.16×10^{-2} | 6.87×10^{-3} |
| CA696 | ABMA | 0 | 3 | 6 | 6 | 4.33×10^{-1} | 2.48×10^{-4} |
| CA630 | JUGR | 1 | 2 | 6 | 7 | 8.14×10^{-2} | 1.16×10^{-2} |
| CA631 | JUGR | 2 | 1 | 6 | 6 | 6.87×10^{-3} | 8.14×10^{-2} |
| CA632 | JUGR | 1 | 2 | 6 | 6 | 8.14×10^{-2} | 6.87×10^{-3} |
| CA698 | JUGR | 1 | 1 | 6 | 7 | 8.14×10^{-2} | 1.09×10^{-1} |
| DGS | JUGR | 1 | 2 | 7 | 6 | 1.09×10^{-1} | 6.87×10^{-3} |
| IVJ | JUGR | 1 | 2 | 6 | 6 | 8.14×10^{-2} | 6.87×10^{-3} |
| KAIM | JUGR | 1 | 2 | 6 | 6 | 8.14×10^{-2} | 6.87×10^{-3} |
| CA677 | PIJE | 2 | 2 | 6 | 6 | 6.87×10^{-3} | 6.87×10^{-3} |
| CA678 | PIJE | 0 | 2 | 6 | 6 | 4.33×10^{-1} | 6.87×10^{-3} |
| DLB | PIJE | 0 | 0 | 6 | 6 | 4.33×10^{-1} | 4.33×10^{-1} |
| IVP | PIJE | 0 | 1 | 6 | 6 | 4.33×10^{-1} | 8.14×10^{-3} |
| LEM | PIJE | 1 | 2 | 6 | 6 | 8.14×10^{-2} | 6.87×10^{-3} |
| LSF | PIJE | 2 | 0 | 6 | 6 | 6.87×10^{-3} | 4.33×10^{-1} |
| LTV | PIJE | 0 | 1 | 6 | 6 | 4.33×10^{-1} | 8.14×10^{-2} |
| SSP | PIJE | 1 | 2 | 6 | 6 | 8.14×10^{-2} | 6.87×10^{-3} |
| CA578 | PIPO | 2 | 2 | 6 | 6 | 6.87×10^{-3} | 6.87×10^{-3} |
| CA583 | PIPO | 1 | 3 | 6 | 6 | 8.14×10^{-2} | 2.48×10^{-4} |
| CA694 | PIPO | 1 | 1 | 6 | 6 | 8.14×10^{-2} | 8.14×10^{-2} |
| CA695 | PIPO | 1 | 3 | 7 | 7 | 1.09×10^{-1} | 5.63×10^{-4} |
| CPRMTR | PIPO | 0 | 2 | 6 | 6 | 4.33×10^{-1} | 6.87×10^{-3} |
| NOD | PIPO | 0 | 1 | 7 | 6 | 4.87×10^{-1} | 8.14×10^{-2} |
| CA576 | TSME | 3 | 3 | 6 | 6 | 2.48×10^{-4} | 2.48×10^{-4} |
| CA692 | TSME | 5 | 1 | 7 | 6 | 5.84×10^{-8} | 8.14×10^{-2} |
| GPH | TSME | 2 | 2 | 7 | 6 | 1.16×10^{-2} | 6.87×10^{-3} |